Dalton Transactions

Accepted Manuscript

This article can be cited before page numbers have been issued, to do this please use: T. Meng, Q. Qin, Z. Chen, H. Zou, K. Wang and F. Liang, *Dalton Trans.*, 2019, DOI: 10.1039/C9DT00866G.

ROYAL SOCIETY OF CHEMISTRY

rsc.li/dalton

View Article Online
DOI: 10.1039/C9DT00866G

Dalton Transactions

ARTICLE

Discovery of a high in vitro and in vivo antitumor activities of organometallic ruthenium(II)-arene complexes with 5,7-dihalogenated-2-methyl-8-quinolinol

Received 00th January 20xx,
Accepted 00th January 20xx

DOI: 10.1039/x0xx00000x

www.rsc.org/

Ting Meng[a], Qi-Pin Qin[a,b,*], Zi-Lu Chen[a], Hua-Hong Zou[a,*], Kai Wang[a,c], and Fu-Pei Liang[a,c,*]

This paper reports the synthesis, structures characterization, and anticancer properties of 13 organometallic Ru(II)-arene complexes: [Ru(η^6-p-cymene)Cl-(L1)] (**1**), [Ru(η^6-p-cymene)Cl-(L2)] (**2**), [Ru(η^6-p-cymene)Cl-(L3)] (**3**), [Ru(η^6-p-cymene)Cl-(L4)] (**4**), [Ru(η^6-p-cymene)Cl-(L5)] (**5**), [Ru(η^6-p-cymene)I-(L1)] (**6**), [Ru(η^6-p-cymene)I-(L2)] (**7**), [Ru(η^6-p-cymene)I-(L3)] (**8**), [Ru(η^6-p-cymene)I-(L4)] (**9**), [Ru(η^6-p-cymene)I-(L5)] (**10**), [Ru(η^6-p-cymene)I-(L6)] (**11**), [Ru(η^6-p-cymene)I-(L7)] (**12**), and [Ru(η^6-p-cymene)Cl-(L8)] (**13**) respectively containing deprotonated 5,7-dichloro-2-methyl-8-quinolinol (H-L1), 5,7-dibromo-2-methyl-8-quinolinol (H-L2), 5-chloro-7-iodo-8-hydroxy-quinoline (H-L3), 5,7-dibromo-8-quinolinol (H-L4), 5,7-diiodo-8-hydroxyquinoline (H-L5), 8-hydroxy-2-methylquinoline (H-L6), 2,8-quinolinediol (H-L7), or 6,7-dichloro-5,8-quinolinedione (H-L8). MTT (3-(4,5-dimethylthiazol-2-yl)-2,5-diphenyltetrazolium bromide) assay showed that 13 organometallic Ru(II)-arene complexes **1**−**13** are more selective for HeLa cells than normal HL-7702 cells. In addition, the **1**, **2**, **5**, and **6**, which contain the active ligands H-L1 and H-L2, showed remarkable cell cytotoxicity, giving the respective IC_{50} values of 2.00 ± 0.20 nM, 0.89 ± 0.62 μM, 25.00 ± 0.30 nM, and 2.18 ± 0.35 μM on HeLa cancer cells. These values indicated higher activity than 6,7-dichloro-5,8-quinolinedione and the other 8-hydroxyquinoline derivative Ru(II)-arene complexes. Interestingly, all these Ru(II)-arene complexes **1**−**13** were significantly less toxic to human hepatic (HL-7702) cells. Moreover, **1**- and **2**-induced HeLa cell apoptosis was mediated by inhibition of telomerase activity and dysfunction of mitochondria, and resulted in DNA damage and increased anti-migration activity on HeLa cells. The organometallic Ru(II)-arene complex **1** exhibited evident priority on antitumor activity than **2**, which should be highly associated with the key roles of the 5,7-dichloro substituted groups in L1 ligand of organometallic Ru(II)-arene complexes **1**. Remarkably, **1** showed higher inhibitory activity against xenograft tumor growth of human cervical cells (HeLa) in vivo (tumor growth inhibition rate (TGIR) = 58.5%) than cisplatin. This study was the first to show that the 5,7-dihalogenated-2-methyl-8-quinolinol organometallic Ru(II)-arene complexes **1** and **2** are novel Ru(II) anticancer drug candidates.

Introduction

Cisplatin and its derivatives (e.g., oxaliplatin, nedaplatin, carboplatin, heptaplatin, and lobaplatin) have remained popular for their anticancer activities to date[1]. Practically, however, the problems of drug resistance and systemic toxicity of Pt-drugs stimulated the design for an alternative transition metal antitumor drugs[1]: NAMI-A[2], DW1/2[3], KP1019[4], RM175[5] and KP1339[4], RAPTA-T[6,7], PTS (RAPTA) complexes[8], [{Ru(phen)$_2$}$_2$tpphz]$^{4+}$,[9] Δ-/Λ-[Ru(phen)$_2$(p-MOPIP)]$^{2+}$ and Λ-/Δ-[Ru(phen)$_2$(p-HPIP)]$^{2+}$ Ru complexes[10], and more recently, several types of nickel(II), copper(II), iron(II,III), ruthenium(II,III), cobalt(II,III), tin(IV), vanadium(IV,V), zinc(II), osmium(VI), rhodium(III), platinum(II,IV), and Ln(III) antitumor metal complexes of 8-hydroxy-quinoline derivatives[11−20]. Turel reported Cl–Ru complex ([Ru(η6-p-cymene)Cl-(Cq)]) induced cell apoptosis via NFκB signaling pathway, which was different from the clioquinol (H-Cq)[16]. A series of Ru(II) coordination complexes with the 2,9-dimethyl-1,10-phenanthroline (or 2,2'-bipyridine) and various hydroxyquinoline mixed chelating ligands were designed but failed to inhibit the proteasome at IC_{50} value[19]. On one hand, Liu investigated 8-hydroxyquinoline [Ru(phen)$_2$(8-HQ)]$^+$ (**PQ**) and [Ru(bpy)$_2$(8-HQ)]$^+$ (**BQ**) ruthenium(II) complexes induce Hep-G2 cell apoptosis via binding of bFGF and remarkably inhibited Hep-G2 tumor growth in vivo[15]. On the other hand, Heidary and coauthors reported that 5-chloro-7-iodo-8-hydroxy-quinoline (H-ClIQ) and 5,7-dibromo-8-quinolinol (H-BrBrQ) Ru(II) complexes exhibited promising cytotoxic activity against HL60 cancer cells, with IC_{50} values of 0.12 ± 0.002 μM and 0.08 ± 2.0 nM, respectively[12]. To date, a highly tumor-selective organometallic Ru(II)-arene complexes with

[a]*State Key Laboratory for the Chemistry and Molecular Engineering of Medicinal Resources, School of Chemistry and Pharmacy, Guangxi Normal University, 15 Yucai Road, Guilin 541004, PR China. E-mail: gxnuchem@foxmail.com (H.-H. Zou); fliangoffce@yahoo.com (F.-P. Liang).*
[b]*Guangxi Key Lab of Agricultural Resources Chemistry and Biotechnology, College of Chemistry and Food Science, Yulin Normal University, 1303 Jiaoyudong Road, Yulin 537000, PR China. qpqin2018@126.com (Q.-P. Qin).*
[c]*Guangxi Key Laboratory of Electrochemical and Magnetochemical Functional Materials, College of Chemistry and Bioengineering, Guilin University of Technology, Guilin 541004, China.*

†Electronic Supplementary Information (ESI) available: The IR and X-ray crystallization data, and **1** suppressed HeLa tumor growth in vivo. The CCDC number for the Ru(II)-arene complexes **1**−**13** and **p-cymene-RuCl** were 1895279, 1895411, 1895280, 1895281, 1895282, 1895283, 1895284, 1895285, 1895412, 1895286, 1895287, 1895288, 1896981 and 1896982. The data can be obtained free of charge *via*http://www.ccdc.cam.ac.uk, or from the Cambridge Crystallographic Data Centre, 12 Union Road, Cambridge CB21EZ, UK (Fax: (+44) 1223-336-033; E-mail: deposit@ccdc.cam.ac.uk). See DOI: 10.1039/x0xx00000x

View Article Online
DOI: 10.1039/C9DT00866G

5,7-dichloro-2-methyl-8-quinolinol (H-MClClQ) and 5,7-dibromo-2-methyl-8-quinolinol (H-MBrBrQ) ligands have yet to be reported, and the detailed in vitro and in vivo anticancer mechanisms of these organometallic Ru(II)-arene complexes remain unexplored.

Therefore, we synthesized the new organometallic Ru(II)-arene complexes ([Ru(η^6-p-cymene)Cl-(L1)] (**1**), [Ru(η^6-p-cymene)Cl-(L2)] (**2**), [Ru(η^6-p-cymene)Cl-(L3)] (**3**), [Ru(η^6-p-cymene)Cl-(L4)] (**4**), [Ru(η^6-p-cymene)Cl-(L5)] (**5**), [Ru(η^6-p-cymene)I-(L1)] (**6**), [Ru(η^6-p-cymene)I-(L2)] (**7**), [Ru(η^6-p-cymene)I-(L3)] (**8**), [Ru(η^6-p-cymene)I-(L4)] (**9**), [Ru(η^6-p-cymene)I-(L5)] (**10**), [Ru(η^6-p-cymene)I-(L6)] (**11**), [Ru(η^6-p-cymene)I-(L7)] (**12**), and [Ru(η^6-p-cymene)Cl-(L8)] (**13**)) with 5,7-dichloro-2-methyl-8-quinolinol (H-L1), 5,7-dibromo-2-methyl-8-quinolinol (H-L2), 5-chloro-7-iodo-8-hydroxy-quinoline (H-L3), 5,7-dibromo-8-quinolinol (H-L4), 5,7-diiodo-8-hydroxyquinoline (H-L5), 8-hydroxy-2-methylquinoline (H-L6), 2,8-quinolinediol (H-L7), or 6,7-dichloro-5,8-quinolinedione (H-L8), respectively. In addition, the Ru(II)-arene complexes **1**- and **2**-induced HeLa cell apoptosis was mediated by inhibition of telomerase activity, dysfunction of mitochondria, and evidently inhibition of HeLa xenograft tumor growth (tumor growth inhibition rate (TGIR) = 58.5%) in vivo.

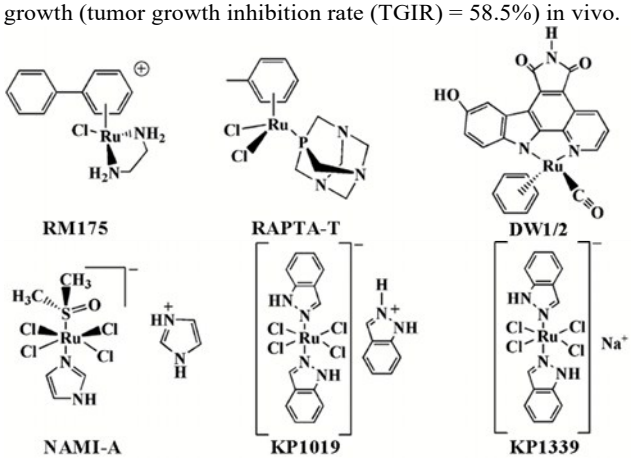

Fig. 1. The chemical structure of anticancer Ru complexes

Results and discussion

Synthesis and characterization

The synthesis of 6,7-dichloro-5,8-quinolinedione (H-L7) was carried out according to a procedure reported by Mulchin and Kubanik et al.[21,22] In addition, 0.049 mmol of dichloro(p-cymene)Ru(II) dimer (**p-cymene-RuCl**) or diiodo(p-cymene)Ru(II) dimer (**p-cymene-RuI**) and 0.098 mmol of 5,7-dichloro-2-methyl-8-quinolinol (H-L1), 5,7-dibromo-2-methyl-8-quinolinol (H-L2), 5-chloro-7-iodo-8-hydroxy-quinoline (H-L3), 5,7-dibromo-8-quinolinol (H-L4), 5,7-diiodo-8-hydroxyquinoline (H-L5), 8-hydroxy-2-methylquinoline (H-L6), 2,8-quinolinediol (H-L7) or 6,7-dichloro-5,8-quinolinedione (H-L8) was dissolved in CH_3OH and CH_2Cl_2 mixture solution, and the solution was refluxed for 6.0 h. The solvent was rotary-evaporated and replaced by CH_3OH, and CH_2Cl_2 mixture solution was removed by filtration. The red-brown precipitate solution of organometallic Ru(II)-arene complexes collected by filtration and washed with n-hexane (5.0 mL, yield: 85.1%–95.2%). Crystals of 13 organometallic Ru(II)-arene complexes **1**–**13** and **p-cymene-RuCl** were obtained by slow evaporation of a CH_3OH and CH_2Cl_2 (v:v = 5:2) solution (Scheme 1) and were suitable for X-ray analysis. All the organometallic Ru(II)-arene complexes were fully characterized by IR spectroscopy, ESI-MS spectra and NMR spectroscopy, single-crystal X-ray diffraction analyses, and elemental analysis (Fig. 1 and S1–S55, Supporting Information).

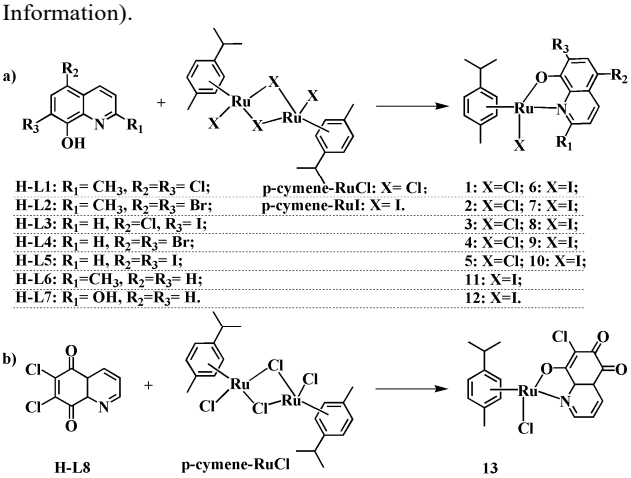

Scheme 1. General synthetic pathway for 13 organometallic Ru(II)-arene complexes **1**–**13**. Reagents and conditions: CH_3OH and CH_2Cl_2 mixture (v:v = 1:1), 65 °C, 6.0 h.

Crystal structure and stability of 13 organometallic Ru(II)-arene complexes 1–13

The 13 organometallic Ru(II)-arene complexes **1**–**13** comprises a Ru(II) center with an η^6-pcymene ring, a deprotonated H-L1, H-L2, H-L3, H-L4, H-L5, H-L6, H-L7, or H-L8 (O^N-QX), and one Cl ligand (Fig. 2, S14–S16 and Table S1–S42). The X-ray diffraction analysis of 13 organometallic Ru(II)-arene complexes revealed that all the 13 organometallic Ru(II)-arene complexes **1**–**13** and **p-cymene-RuCl** also featured the pseudo-tetrahedral piano stool structure (Figs. 2 and S14–S16) with the Ru(II) atom center coordinated to the pyridine N atom (N^ligand) and the adjacent O atom (O^ligand) in a bidentate fashion.

Furthermore, the solution behavior of 13 organometallic Ru(II)-arene complexes **1**–**13** (3.0×10^{-5} M) in 10 mM Tris-HCl buffer (pH = 7.35, TBS, containing 5% DMSO) or DMSO solution was further studied by ESI-MS spectra and NMR spectroscopy. The NMR result showed that no other peaks appeared (Figs. S31–S55), indicating no structural transitions and/or decompositions on the 13 organometallic Ru(II)-arene complexes **1**–**13**. The ESI-MS assay suggested that the ESI-MS of 13 organometallic Ru(II)-arene complexes **1**–**13** (3.0×10^{-5} M) had the base peak for $[M - Cl]^+$ at m/z = 463.4, $[M - Cl + DMSO]^+$ at m/z = 626.9, $[M - Cl]^+$ at m/z = 539.4, $[M - Cl]^+$ at

View Article Online
DOI: 10.1039/C9DT00866G

m/z = 537.3, $[M - Cl]^+$ at *m/z* = 631.3, $[M - Cl]^+$ at *m/z* = 461.4, $[M - Cl]^+$ at *m/z* = 551.4, $[M - Cl]^+$ at *m/z* = 539.4, $[M - Cl]^+$ at *m/z* = 537.3, $[M - Cl]^+$ at *m/z* = 631.3, $[M - Cl]^+$ at *m/z* = 393.4, $[M - Cl]^+$ at *m/z* = 395.4 and $[M - Cl]^+$ at *m/z* = 463.5 in the TBS for 0 h (Figs. S17–S30), respectively. No change in the m/z values (Figs. S17–S30) was observed after 48-h incubation in 10 mM Tris-HCl buffer (pH = 7.35, TBS), suggesting that 13 organometallic Ru(II)-arene complexes **1**−**13** were stable under this condition. In conclusion, 13 organometallic Ru(II)-arene complexes **1**−**13** (3.0×10^{-5} M) were stable in 10 mM TBS for 48 h at 37 °C.

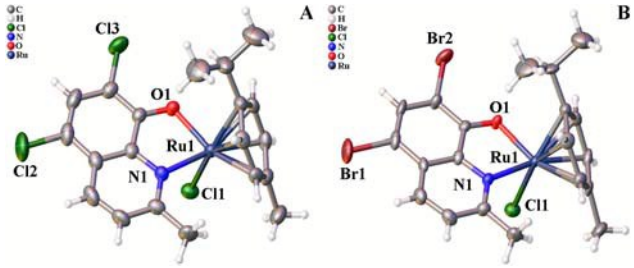

Fig. 2. Molecular structure of organometallic Ru(II)-arene complexes **1** (A) and **2** (B), respectively.

In vitro cytotoxicity

MTT assays with HeLa (human cervical cancer), T-24 (human bladder cancer), SK-OV-3 (human ovarian carcinoma cancer), and HL-7702 normal cells were performed to evaluate the antitumor activity of 13 organometallic Ru(II)-arene complexes **1**−**13**, H-L1, H-L2, H-L3, H-L4, H-L5, H-L6, H-L7, H-L8, and cisplatin. Table 1 revealed that organometallic Ru(II)-arene complexes **1** and **2** showed stronger antitumor potency than 11 organometallic Ru(II)-arene complexes and their corresponding H-L1, H-L2, H-L3, H-L4, H-L5, H-L6, H-L7, and H-L8 ligands, and the in vitro different antitumor activity were in the following order: **1** > **2** > **3** > **4** > **5** > **13**, **6** > **7** > **8** > **9** > **10**, and **1** > **2** > **11** > **12**. In addition, **1** was most cytotoxicities in HeLa cells, with IC_{50} values 2.00 ± 0.20 nM, which was 40.0−9010.0 times more potent than that of clinical medicine cisplatin (IC_{50} = 15.02 ± 1.85 μM), 5,7-dichloro-2-methyl-8-quinolinol Fe(III) complex (IC_{50} = 5.04 ± 0.62 μM)[17], 5-chloro-7-iodo-8-hydroxy-quinoline (H-ClIQ) and 5,7-dibromo-8-quinolinol Pt(II), and Dy(III) and Ru(II) complexes (IC_{50} = 5.02 ± 0.62 μM, 4.09 ± 1.06 μM, 1.53 ± 0.59 μM, 18.02 ± 1.05 μM, 0.12 ± 0.002 μM, and 0.08 ± 2.0 μM)[12,18,20]. Interestingly, these Ru(II)-arene complexes **1** and **2** were significantly less toxic to HL-7702 normal cells (IC_{50} > 100 μM), indicating the selectivity of Ru(II)-arene complexes **1** and **2** on HeLa. This study was the first report to show that 5,7-dihalogenated-2-methyl-8-quinolinol organometallic Ru(II)-arene complexes **1** and **2** were remarkably cytotoxic to HeLa tumor cells but significantly less toxic to HL-7702 normal cells.

Table 1. Cytotoxicities (IC_{50}, μM) of 13 organometallic Ru(II)-arene complexes (H-L1, H-L2, H-L3, H-L4, H-L5, H-L6, H-L7, H-L8) and cisplatin toward human HeLa, T-24, SK-OV-3, and HL-7702 cell lines[a]

Compounds	HeLa	T-24	SK-OV-3	HL-7702
H-L1	> 100	> 100	65.36 ± 1.69	> 100
1	2.00 ± 0.20 nM[c]	2.69 ± 0.74	1.03 ± 0.52	> 100
6	0.89 ± 0.62	5.36 ± 1.09	2.15 ± 1.13	> 100
H-L2	> 100	75.03 ± 1.02	82.23 ± 1.22	88.96 ± 0.45
2	25.00 ± 0.30 nM[c]	8.36 ± 0.11	2.03 ± 0.51	> 100
7	2.18 ± 0.35	11.25 ± 0.63	2.55 ± 0.76	> 100
H-L3	50.26 ± 0.58	25.03 ± 1.01	15.06 ± 0.77	75.25 ± 1.43
3	4.43 ± 0.52	20.81 ± 1.45	3.19 ± 1.06	85.69 ± 1.02
8	8.31 ± 1.17	> 100	6.10 ± 0.97	49.03 ± 0.75
H-L4	54.03 ± 1.18	71.29 ± 2.06	88.01 ± 1.65	> 100
4	4.96 ± 0.39	20.31 ± 0.33	3.65 ± 0.46	77.69 ± 0.36
9	8.95 ± 0.76	32.92 ± 1.25	6.83 ± 1.11	65.97 ± 0.86
H-L5	86.99 ± 1.85	> 100	97.56 ± 1.28	75.03 ± 1.09
5	5.73 ± 0.44	7.19 ± 0.23	4.44 ± 0.63	80.12 ± 0.28

View Article Online
DOI: 10.1039/C9DT00866G

10	9.36 ± 1.45	13.99 ± 1.02	7.22 ± 0.59	70.15 ± 1.36
H-L8	35.06 ± 1.44	28.11 ± 0.57	40.23 ± 1.33	60.36 ± 2.21
13	10.53 ± 0.19	17.83 ± 1.45	16.57 ± 0.58	61.23 ± 0.74
H-L6	90.22 ± 0.55	85.03 ± 1.01	57.32 ± 0.35	89.63 ± 1.52
11	6.11 ± 0.56	10.09 ± 1.85	4.36 ± 0.69	88.23 ± 1.56
H-L7	70.14 ± 1.21	61.85 ± 0.74	65.82 ± 1.16	77.98 ± 1.08
12	2.03 ± 0.22	5.01 ± 1.07	6.17 ± 0.15	90.22 ± 1.73
Cisplatin[b]	15.02 ± 1.85	16.36 ± 0.95	12.23 ± 0.41	16.09 ± 1.05

[a]Cancer and normal cells were treated with 13 organometallic Ru(II)-arene complexes, the corresponding ligands, and cisplatin at different concentrations for 48 h. IC_{50} values were equal to the mean value ± SD value from five independent assays. [b]A total of 1.0 mM cisplatin was prepared in 0.154 M NaCl[23–26]. [c]The concentration was in nM.

Migration assay

Cancer cell migration was an important characteristic in cancer metastasis[27,28]. The transwell migration assay in vitro was performed on HeLa cells to study anti-migration effect of organometallic Ru(II)-arene complexes **1** (2.0 nM) and **2** (25.0 nM). The organometallic Ru(II)-arene complexes **1** (2.0 nM) and **2** (25.0 nM) showed excellent anti-migration activities on HeLa cells at 2.0 nM (low concentrations) (Fig. 3). Results indicated that organometallic Ru(II)-arene complex **1** (2.0 nM) more significantly inhibited HeLa cancer cell migration at 2.0 nM than that of **2** (25.0 nM).

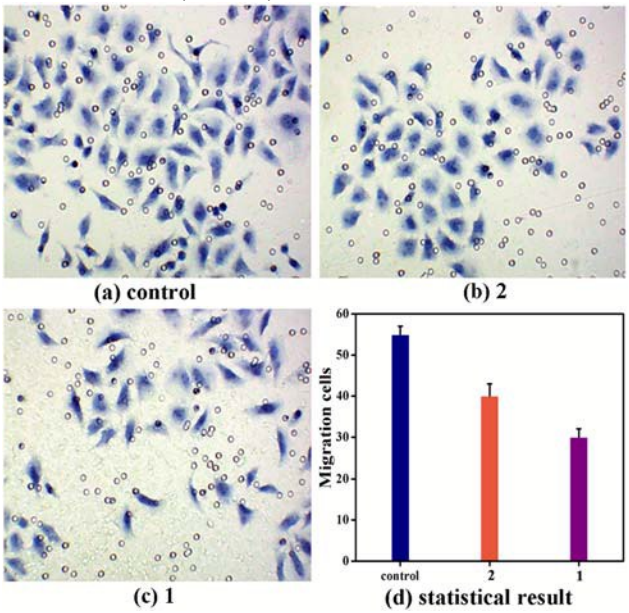

Fig. 3. Anti-migration effect of organometallic Ru(II)-arene complexes **1** (2.0 nM, c) and **2** (25.0 nM, b) on HeLa cells (a) for 24 h via transwell migration assay. (d) The statistical result of anti-migration assays were equal to the mean value ± SD value from three independent assays (magnification 200 ×)

1- and 2-Induced Apoptosis

HeLa cells incubated with organometallic Ru(II)-arene complexes **1** (2.0 nM) and **2** (25.0 nM) for 24 h exhibited significant G0 peaks (sub-G1 peaks), which indicated HeLa cell apoptosis and the apoptotic peaks of 26.54% and 18.68% in sub-G1 phase of the cell cycle distribution, respectively (Fig. 4a–c). Such is the result further verified in the apoptosis experiment by flow cytometry with FITC-Annexin V and PI (propidium iodide) double staining. HeLa tumor cells were treated with organometallic Ru(II)-arene complexes **1** (2.0 nM) and **2** (25.0 nM) for 24 h, and then these cancer cells were harvested and analyzed by flow cytometry after staining with PI and Annexin V-FITC dye (Fig. 4d–f) to confirm this property. The percentages of apoptosis cells were 28.30% and 19.55%, respectively, when the HeLa cancer cells were incubated with organometallic Ru(II)-arene complexes **1** (2.0 nM) and **2** (25.0 nM) for 24 h.

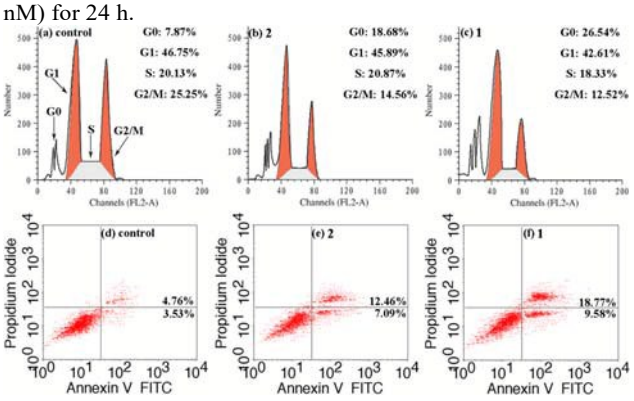

Fig. 4. The organometallic Ru(II)-arene complexes **1** (2.0 nM) and **2** (25.0 nM) induced the cell cycle distribution (a–c) and apoptosis (d–f) of HeLa cells for 24 h

1 and 2 caused DNA damage and mitochondrial dysfunction

H2A.X and cleaved PARP proteins were closely related to DNA damage response factors[29–32]. Organometallic Ru(II)-arene complexes **1** (2.0 nM) and **2** (25.0 nM) treatment were suggested to induce HeLa cell apoptosis, which was highly associated with DNA damage or the appearance of sub-G1 peak (the hypodiploid DNA content peak)[29–32]. Therefore, the

View Article Online
DOI: 10.1039/C9DT00866G

immunofluorescence assay and Western blot were used to clarify the expression of the H2A.X and cleaved-PARP proteins in the HeLa cells. Treatment of organometallic Ru(II)-arene complexes **1** (2.0 nM) and **2** (25.0 nM) remarkably enhanced the levels of H2A.X and cleaved-PARP proteins expression (Figs. 5 and 6). Thus, our data suggested that organometallic Ru(II)-arene complexes **1** (2.0 nM) and **2** (25.0 nM) substantially induced DNA damage. Moreover, Bcl-2 family apoptosis-related proteins (e.g., bad, bcl-2, and bax) and mitochondria-mediated pathway (e.g., cytochrome c, caspase-3, and caspase-9) were activated by DNA damage[29,33–35]. Further evidence from Western blot suggested that organometallic Ru(II)-arene complexes **1** (2.0 nM) and **2** (25.0 nM) upregulated the expression of bad and bax proteins and the correspondingly downregulated the level of bcl-2 protein (Fig. 6). These stimuli could decrease the ΔΨm (mitochondrial membrane potential (MMP)) level (Fig. 7), and the correspondingly green fluorescence intensity (JC-1 monomers) increases from 8.76% to 45.51% or 36.65%, respectively, which also could activate the level of reactive oxygen species (ROS) (Fig. 8 and Table S43) and increase the apoptotic cytochrome c and active caspase-3 and caspase-9 proteins (Fig. 6) in HeLa cells.

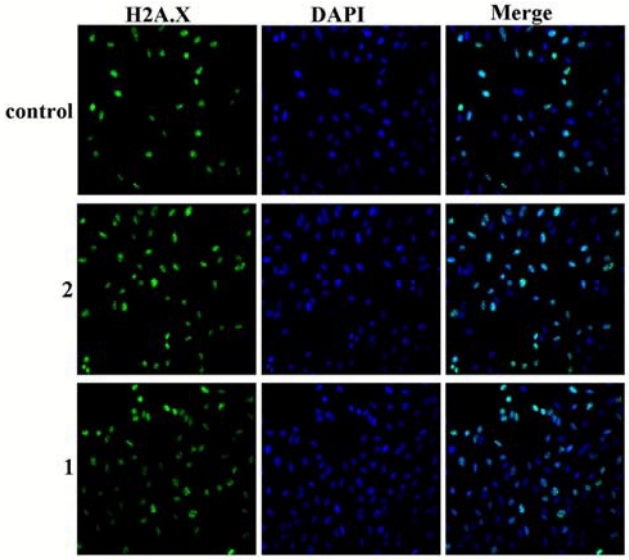

Fig. 5. The organometallic Ru(II)-arene complexes **1** (2.0 nM) and **2** (25.0 nM) induced DNA damage in HeLa cells for 24 h. The HeLa cells were treated with organometallic Ru(II)-arene complexes **1** (2.0 nM) and **2** (25.0 nM) for 24 h, respectively, and followed staining by H2A.X (green, primary antibodies) and DAPI (blue) for 40.0 min. Thereafter, these cancer cells were visualized by LeicaTCS-SP5 confocal microscope (Germany, magnification 400 ×).

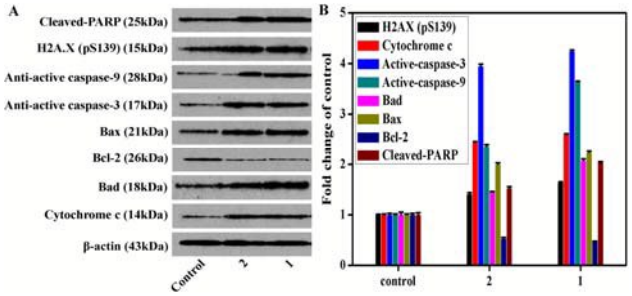

Fig. 6. (A and B) Western blot analysis to detect the levels of the DNA damage, mitochondria-mediated pathway, and Bcl-2 family-related proteins in HeLa cells treated with organometallic Ru(II)-arene complexes **1** (2.0 nM) and **2** (25.0 nM) for 24 h

1 and 2 inhibit telomerase activity and decreased the related proteins

Previous studies demonstrated that the cell cycle distribution in sub-G1 phase by organometallic Ru(II)-arene complexes **1** (2.0 nM) and **2** (25.0 nM) was treated, which was related to the inhibition of telomerase[36–39]. First, the effect of organometallic Ru(II)-arene complexes **1** (2.0 nM) and **2** (25.0 nM) on telomerase in HeLa cells was determined. Fig. 9A showed that organometallic Ru(II)-arene complexes **1** (2.0 nM) and **2** (25.0 nM) evidently inhibited telomerase activity (i.e., 49.51% and 30.61%, respectively). As predicted, organometallic Ru(II)-arene complexes **1** (2.0 nM) and **2** (25.0 nM) significantly decreased the level of the related (e.g., c-myc and hTERT) proteins in HeLa cells (Fig. 9B and C). Results clearly revealed that organometallic Ru(II)-arene complexes **1** (2.0 nM) may have higher affinity toward telomerase activity and the related proteins than **2** (25.0 nM), which was in accord with the above results.

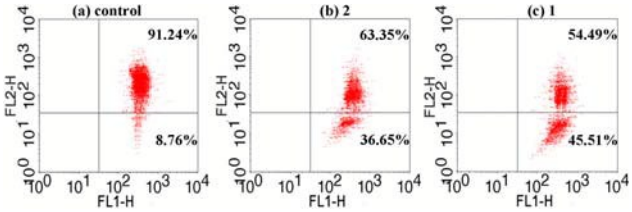

Fig. 7. The organometallic Ru(II)-arene complexes **1** (2.0 nM) and **2** (25.0 nM) decreased the ΔΨm of HeLa cells for 24 h and consequently were analyzed by flow cytometry after incubation with JC-1 staining (the fluorescence probe JC-1) for 30.0 min

View Article Online
DOI: 10.1039/C9DT00866G

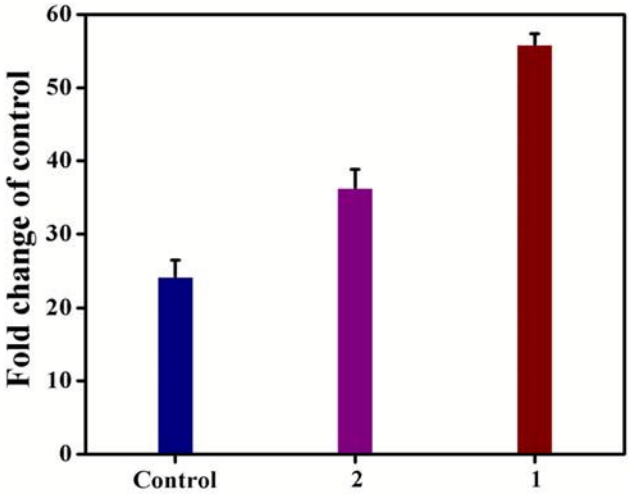

Fig. 8. The organometallic Ru(II)-arene complexes **1** (2.0 nM) and **2** (25.0 nM) which increased the level of ROS generation in HeLa cells for 24.0 h were analyzed by fluorescence photometer

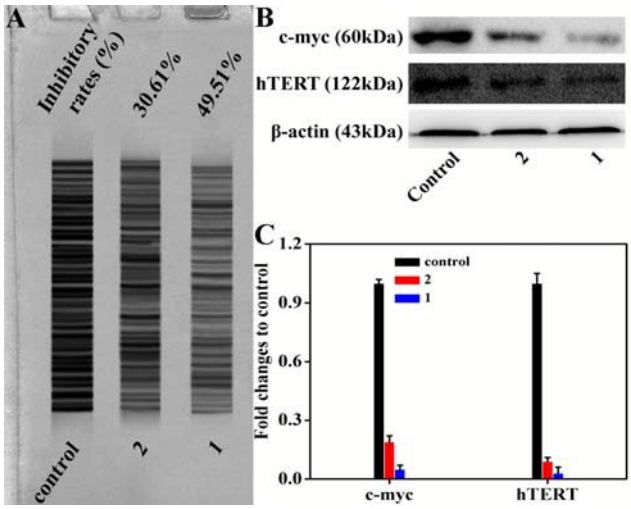

Fig. 9. The organometallic Ru(II)-arene complexes **1** (2.0 nM) and **2** (25.0 nM) inhibit telomerase activity and the related proteins. (A) The influence of organometallic Ru(II)-arene complexes **1** (2.0 nM) and **2** (25.0 nM) on the telomerase activity of HeLa. (B and C) Western blot analysis of the related (e.g., c-myc and hTERT) proteins in organometallic Ru(II)-arene complexes **1** (2.0 nM) and **2** (25.0 nM) treated cells for 24 h

1 suppressed HeLa tumor growth in vivo

Model nude mice with HeLa tumor received a possible highest administration value of organometallic Ru(II)-arene complex **1** (10.0 mg/kg every two days (q2d), 1.0 mL/20 g, 5% v/v DMSO/saline) by intraperitoneal injection[40–42], and no signs of peritonitis (other adverse effects) or damage to organs were observed, suggesting that organometallic Ru(II)-arene complex **1** (10.0 mg/kg/q2d) shows no significant toxicity within the 21-day treatment. Fig. 10 and Tables S44−S46 show that treatment with organometallic Ru(II)-arene complex **1** (10.0 mg/kg/q2d) resulted in a significant reduction in tumor volume (T/C = 35.6%) in comparison with the vehicle group. In addition, inhibition of HeLa TGIR by organometallic Ru(II)-arene complex **1** (10.0 mg/kg/q2d) with treated versus vehicle group of 58.5% was observed on day 21.0 after treatment, which was significantly higher than that of cisplatin (35.2%)[43]. The data testified more potent inhibitory effect of organometallic Ru(II)-arene complex **1** (10.0 mg/kg/q2d) on HeLa tumor growth (TGIR = 58.5%) in vivo and higher safety than cisplatin.

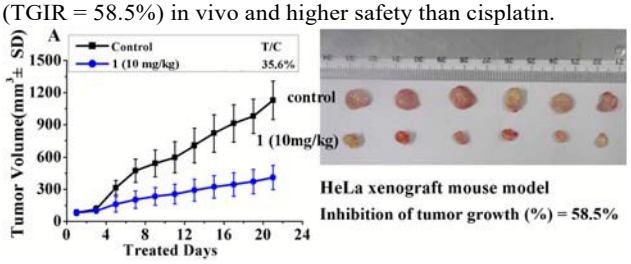

Fig. 10. The organometallic Ru(II)-arene complex **1** suppressed HeLa tumor growth in vivo. Effect (A) and photographs (B) of organometallic Ru(II)-arene complex **1** (10 mg/kg/q2d) and vehicle (10% DMSO in saline, v/v) on HeLa tumor growth (mean tumor volume (mm^3)) ± SD (n = 6)

Structure–Activity Relationships (SAR)

Certain SARs trends in the different substituted quinolinedione and 8-hydroxyquinoline derivative ligands, and the differences antitumor activities (Fig. 11) and their mechanisms were observed based on the in vitro and in vivo anticancer activity results of 13 organometallic Ru(II)-arene complexes **1**−**13**.

i) The in vitro different cytotoxicity studies were in the following order: **1** > **2** > **3** > **4** > **5** > **13**, **6** > **7** > **8** > **9** > **10** and **1** > **2** > **11** > **12**.

ii) The in vitro antitumor activity of organometallic Ru(II)-arene complexes **1** and **2** follow the order of **1** > **2**.

iii) The in vivo anticancer activity of organometallic Ru(II)-arene complex **1** and cisplatin in HeLa tumor xenograft (SARs trend **1** > cisplatin) was also observed.

View Article Online
DOI: 10.1039/C9DT00866G

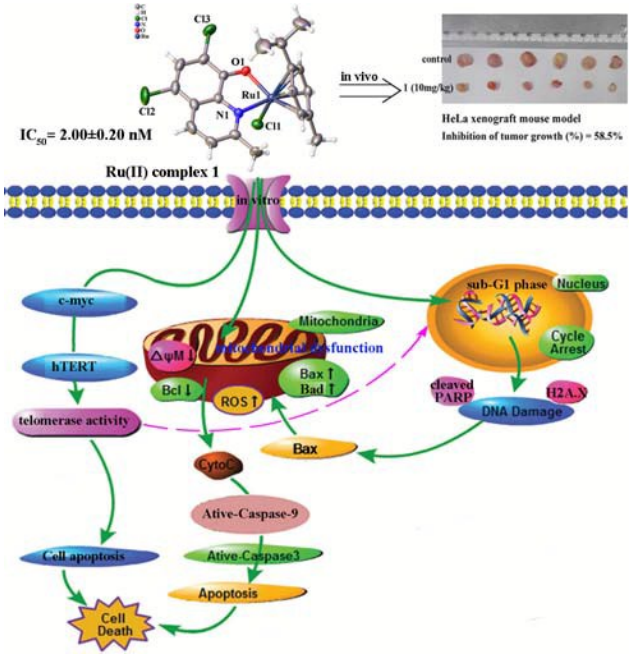

Fig. 11. Proposed anticancer mechanisms for organometallic Ru(II)-arene complexes **1** and **2** (e.g., mechanisms of **1**)

Experimental materials and methods

Synthesis of 6,7-dichloro-5,8-quinolinedione (L7)

The synthesis of 6,7-dichloro-5,8-quinolinedione (L7) was carried out according to a procedure reported by Mulchin and Kubanik et al.[21,22] Yield: 17.0%. ESI-MS: m/z = 241.2 for $[M + Na]^+$. Elemental analysis: calcd (%) for $C_9H_5Cl_2NO_2$: C 46.99, H 2.19, N 6.09; found: C 46.95, H 2.21, N 6.06. ^{1}H NMR (500 MHz, DMSO-d_6) δ 9.05 (dd, J = 4.6, 1.7 Hz, 1H), 8.46 (dd, J = 7.9, 1.7 Hz, 1H), 7.89 (dd, J = 7.9, 4.6 Hz, 1H). ^{13}C NMR (126 MHz, DMSO-d_6) δ 176.46, 174.71, 154.93, 147.52, 143.59, 142.04, 135.38, 128.99, 128.75.

Synthesis and characterization of 13 organometallic Ru(II)-arene complexes

A total of 0.049 mmol of dichloro(p-cymene) Ru(II) dimer (**p-cymene-RuCl**) or diiodo(p-cymene) Ru(II) dimer (**p-cymene-RuI**) and 0.098 mmol of 5,7-dichloro-2-methyl-8-quinolinol (H-L1), 5,7-dibromo-2-methyl-8-quinolinol (H-L2), 5-chloro-7-iodo-8-hydroxy-quinoline (H-L3), 5,7-dibromo-8-quinolinol (H-L4), 5,7-diiodo-8-hydroxyquinoline (H-L5), 8-hydroxy-2-methylquinoline (H-L6), 2,8-quinolinediol (H-L7), or 6,7-dichloro-5,8-quinolinedione (H-L8) were dissolved in 10.0 mL of CH_3OH/CH_2Cl_2 mixture (v:v = 1:1), and the solution was refluxed for 6.0 h. The solvent was rotary evaporated, replaced by CH_3OH/CH_2Cl_2 (5.0 mL, v:v = 1:1), and was removed by filtration. The red-brown precipitate solution of organometallic Ru(II)-arene complexes were collected by filtration and washed with n-hexane (5.0 mL, yield: 85.1%–95.2%). Crystals of 13 organometallic Ru(II)-arene complexes **1**–**13** suitable for X-ray analysis were obtained by slow evaporation of a CH_3OH/CH_2Cl_2 (6.0 mL, v:v = 5:2) solution (Scheme 1).

*Data for **6**:* Yield (95.2%). Elemental analysis calcd (%) for $C_{20}H_{20}Cl_2INORu$: C 40.77, H 3.42, N 2.38. Found: C 40.72, H 3.45, N 2.34. ESI-MS: m/z = 461.4 for $[M – Cl]^+$. ^{1}H NMR (500 MHz, DMSO-d_6) δ 8.22 (d, J = 8.6 Hz, 1H), 7.67 (d, J = 8.7 Hz, 1H), 7.51 (s, 1H), 5.95 (d, J = 5.9 Hz, 1H), 5.87 – 5.80 (m, 2H), 5.55 (d, J = 5.9 Hz, 1H), 3.14 (s, 3H), 2.65 (dq, J = 13.9, 6.9 Hz, 1H), 2.47 (s, 3H), 1.09 (d, J = 6.9 Hz, 3H), 0.93 (d, J = 6.9 Hz, 3H). ^{13}C NMR (126 MHz, DMSO-d_6) δ 163.06, 162.75, 144.85, 134.30, 128.06, 125.48, 124.26, 117.64, 110.37, 104.15, 98.48, 85.38, 81.48, 80.69, 80.38, 31.13, 30.31, 22.19, 21.82, 21.05.

*Data for **1**:* Yield (85.1%). Elemental analysis calcd (%) for $C_{20}H_{20}Cl_3NORu$: C 48.25, H 4.05, N 2.81. Found: C 48.28, H 4.07, N 2.78. ESI-MS: m/z = 463.4 for $[M – Cl]^+$. ^{1}H NMR (500 MHz, DMSO-d_6) δ 8.20 (d, J = 8.6 Hz, 1H), 7.74 (s, 1H), 7.69 (d, J = 8.7 Hz, 1H), 5.98 (dd, J = 5.9, 1.1 Hz, 1H), 5.88 (dd, J = 6.1, 1.2 Hz, 1H), 5.77 (dd, J = 6.2, 1.2 Hz, 1H), 5.55 (dd, J = 5.9, 1.2 Hz, 1H), 3.32 (s, 1H), 3.19 (s, 3H), 2.20 (s, 3H), 1.04 (d, J = 7.0 Hz, 3H), 0.91 (d, J = 6.9 Hz, 3H). ^{13}C NMR (126 MHz, DMSO-d_6) δ 162.68, 161.18, 143.94, 133.80, 127.60, 124.96, 123.72, 116.58, 109.83, 100.39, 100.10, 86.31, 79.87, 79.78, 78.47, 30.25, 28.25, 21.64, 21.54, 18.27

*Data for **2**:* Yield (87.5%). Elemental analysis calcd (%) for $C_{20}H_{20}Br_2ClNORu$: C 40.94, H 3.44, N 2.39. Found: C 40.90, H 3.47, N 2.36. ESI-MS: m/z = 626.9 for $[M – Cl + DMSO]^+$. ^{1}H NMR (500 MHz, DMSO-d_6) δ 8.20 (d, J = 8.6 Hz, 1H), 7.74 (s, 1H), 7.69 (d, J = 8.7 Hz, 1H), 5.98 (dd, J = 5.9, 1.1 Hz, 1H), 5.88 (dd, J = 6.1, 1.1 Hz, 1H), 5.77 (dd, J = 6.1, 1.2 Hz, 1H), 5.55 (dd, J = 5.9, 1.2 Hz, 1H), 3.19 (s, 3H), 2.20 (s, 3H), 1.04 (d, J = 7.0 Hz, 3H), 0.91 (d, J = 6.9 Hz, 3H). ^{13}C NMR (126 MHz, DMSO-d_6) δ 164.87, 161.71, 156.92, 144.33, 136.84, 133.52, 125.88, 107.31, 100.79, 100.75, 99.41, 86.80, 80.51, 80.37, 79.36, 30.82, 28.79, 22.19, 22.15, 18.82.

*Data for **7**:* Yield (90.1%). Elemental analysis calcd (%) for $C_{20}H_{20}Br_2INORu$: C 35.42, H 2.97, N 2.07. Found: C 35.45, H 2.94, N 2.02. ESI-MS: m/z = 551.4 for $[M – Cl]^+$. ^{1}H NMR (500 MHz, DMSO-d_6) δ 8.15 (d, J = 8.6 Hz, 1H), 7.73 (s, 1H), 7.68 (d, J = 8.7 Hz, 1H), 5.93 (dd, J = 5.9, 1.2 Hz, 1H), 5.86 (dd, J = 6.3, 1.2 Hz, 1H), 5.83 – 5.81 (m, 1H), 5.56 (dd, J = 6.0, 1.2 Hz, 1H), 3.15 (s, 3H), 2.65 (p, J = 7.0 Hz, 1H), 2.46 (s, 3H), 1.10 (d, J = 7.0 Hz, 3H), 0.93 (d, J = 6.9 Hz, 3H). ^{13}C NMR (126 MHz, DMSO-d_6) δ 164.66, 162.69, 144.63, 136.75, 133.39, 125.98, 125.80, 107.73, 104.31, 99.37, 98.17, 85.17, 81.68, 81.05, 80.29, 31.09, 30.29, 22.25, 21.76, 20.95.

*Data for **13**:* Yield (93.5%). Elemental analysis calcd (%) for $C_{19}H_{19}Cl_2NO_3Ru$: C 47.41, H 3.98, N 2.91. Found: C 47.36, H 4.03, N 2.88. ESI-MS: m/z = 463.5 for $[M – Cl]^+$. ^{1}H NMR (500 MHz, DMSO-d_6) δ 9.44 (d, J = 5.6 Hz, 1H), 8.32 (d, J = 7.8 Hz, 1H), 7.83 (dd, J = 7.8, 5.6 Hz, 1H), 6.07 (d, J = 6.1 Hz, 1H), 6.02 (d, J = 6.0 Hz, 1H), 5.85 (d, J = 6.2 Hz, 1H), 5.84 – 5.79 (m, 2H), 2.77 (q, J = 6.9 Hz, 1H), 2.20 (s, 3H), 1.21 (d, J = 7.0 Hz, 3H), 1.17 (s, 3H).

*Data for **3**:* Yield (89.6%). Elemental analysis calcd (%) for $C_{19}H_{18}Cl_2INORu$: C 39.67, H 3.15, N 2.43. Found: C 39.63,

View Article Online
DOI: 10.1039/C9DT00866G

H 3.19, N 2.41. ESI-MS: m/z = 539.4 for $[M - Cl]^+$. ^{1}H NMR (500 MHz, DMSO-d_6) δ 9.30 (dd, J = 4.9, 1.3 Hz, 1H), 8.36 (dd, J = 8.6, 1.2 Hz, 1H), 7.79 (s, 1H), 7.71 (dd, J = 8.6, 4.9 Hz, 1H), 5.92 (dd, J = 6.1, 1.1 Hz, 1H), 5.78 (dd, J = 6.0, 1.1 Hz, 1H), 5.71 (dd, J = 6.0, 1.1 Hz, 1H), 5.64 (dd, J = 6.1, 1.1 Hz, 1H), 2.71 (hept, J = 6.9 Hz, 1H), 2.19 (s, 3H), 1.17 (d, J = 6.9 Hz, 3H), 1.09 (d, J = 6.9 Hz, 3H). ^{13}C NMR (126 MHz, DMSO-d_6) δ 167.73, 152.06, 141.96, 136.23, 134.52, 127.01, 124.37, 111.02, 101.17, 97.92, 82.60, 82.51, 82.15, 80.70, 80.35, 30.94, 22.31, 22.28, 18.41.

*Data for **4**:* Yield (92.3%). Elemental analysis calcd (%) for $C_{19}H_{18}Br_2ClNORu$: C 39.85, H 3.17, N 2.45. Found: C 39.81, H 3.20, N 2.43. ESI-MS: m/z = 537.3 for $[M - Cl]^+$. ^{1}H NMR (500 MHz, DMSO-d_6) δ 9.33 (dd, J = 5.0, 1.2 Hz, 1H), 8.31 (dd, J = 8.6, 1.2 Hz, 1H), 7.81 (s, 1H), 7.72 (dd, J = 8.6, 5.0 Hz, 1H), 5.96 – 5.90 (m, 1H), 5.83 (dd, J = 6.1, 1.2 Hz, 1H), 5.71 – 5.63 (m, 2H), 2.69 (p, J = 6.9 Hz, 1H), 2.18 (s, 3H), 1.13 (d, J = 6.9 Hz, 3H), 1.08 (d, J = 6.9 Hz, 3H). ^{13}C NMR (126 MHz, DMSO-d_6) δ 164.73, 151.63, 143.87, 136.27, 133.97, 127.15, 123.96, 105.98, 100.48, 98.60, 97.87, 82.21, 81.72, 81.38, 79.95, 30.35, 21.80, 21.55, 17.89.

*Data for **9**:* Yield (88.3%). Elemental analysis calcd (%) for $C_{19}H_{18}Br_2INORu$: C 34.36, H 2.73, N 2.11. Found: C 34.40, H 2.71, N 2.13. ESI-MS: m/z = 537.3 for $[M - Cl]^+$. ^{1}H NMR (500 MHz, DMSO-d_6) δ 9.28 (dd, J = 5.0, 1.2 Hz, 1H), 8.28 (dd, J = 8.6, 1.2 Hz, 1H), 7.80 (s, 1H), 7.69 (dd, J = 8.6, 5.0 Hz, 1H), 5.87 (dd, J = 6.1, 1.2 Hz, 1H), 5.84 (dd, J = 6.0, 1.3 Hz, 1H), 5.79 (dd, J = 6.0, 1.2 Hz, 1H), 5.72 (dd, J = 5.9, 1.2 Hz, 1H), 2.83 – 2.78 (m, 1H), 2.33 (s, 3H), 1.17 (d, J = 7.0 Hz, 3H), 1.12 (d, J = 6.9 Hz, 3H). ^{13}C NMR (126 MHz, DMSO-d_6) 164.50, 152.86, 144.33, 136.15, 133.86, 127.07, 124.03, 106.27, 103.23, 98.48, 96.10, 83.12, 81.52, 81.22, 81.00, 30.74, 21.75, 21.54, 19.10.

*Data for **5**:* Yield (87.0%). Elemental analysis calcd (%) for $C_{19}H_{18}ClI_2INORu$: C 34.23, H 2.72, N 2.10. Found: C 34.20, H 2.75, N 2.08. ESI-MS: m/z = 631.3 for $[M - Cl]^+$. ^{1}H NMR (500 MHz, DMSO-d_6) δ 9.25 (dd, J = 4.9, 1.2 Hz, 1H), 8.16 (dd, J = 8.6, 1.2 Hz, 1H), 8.06 (s, 1H), 7.68 (dd, J = 8.6, 4.9 Hz, 1H), 5.92 (dd, J = 6.1, 1.2 Hz, 1H), 5.77 (dd, J = 5.9, 1.2 Hz, 1H), 5.70 (dd, J = 5.9, 1.2 Hz, 1H), 5.64 (dd, J = 6.1, 1.2 Hz, 1H), 2.70 (hept, J = 6.9 Hz, 1H), 2.19 (s, 3H), 1.17 (d, J = 6.9 Hz, 3H), 1.08 (d, J = 7.0 Hz, 3H). ^{13}C NMR (126 MHz, DMSO-d_6) δ 168.92, 151.98, 145.55, 142.86, 141.31, 131.02, 124.89, 101.15, 97.91, 83.15, 82.64, 82.54, 82.11, 80.74, 73.45, 30.94, 22.33, 22.29, 18.43.

*Data for **10**:* Yield (91.0%). Elemental analysis calcd (%) for $C_{19}H_{18}I_3INORu$: C 30.10, H 2.39, N 2.11. Found: C 30.05, H 2.43, N 2.09. ESI-MS: m/z = 631.3 for $[M - Cl]^+$. ^{1}H NMR (500 MHz, DMSO-d_6) δ 9.20 (dd, J = 4.9, 1.2 Hz, 1H), 8.12 (dd, J = 8.6, 1.2 Hz, 1H), 8.05 (s, 1H), 7.65 (dd, J = 8.6, 5.0 Hz, 1H), 5.86 (dd, J = 6.1, 1.3 Hz, 1H), 5.79 (td, J = 6.5, 1.2 Hz, 2H), 5.73 (dd, J = 6.0, 1.2 Hz, 1H), 2.81 (p, J = 6.9 Hz, 1H), 2.33 (s, 3H), 1.22 (d, J = 7.0 Hz, 3H), 1.13 (d, J = 6.9 Hz, 4H). ^{13}C NMR (126 MHz, DMSO-d_6) δ 168.70, 153.23, 145.43, 143.32, 141.20, 130.94, 124.94, 103.93, 96.17, 84.19, 83.33, 82.06, 81.97, 81.33, 73.39, 31.31, 22.31, 22.12, 19.57.

*Data for **8**:* Yield (88.9%). Elemental analysis calcd (%) for $C_{19}H_{18}Cl_2INORu$: C 34.23, H 2.72, N 2.10. Found: C 34.19, H 2.74, N 2.07. ESI-MS: m/z = 539.4 for $[M - Cl]^+$. ^{1}H NMR (500 MHz, DMSO-d_6) δ 9.25 (dd, J = 5.0, 1.3 Hz, 1H), 8.32 (dd, J = 8.6, 1.2 Hz, 1H), 7.78 (s, 1H), 7.68 (dd, J = 8.6, 5.0 Hz, 1H), 5.86 (dd, J = 6.0, 1.2 Hz, 1H), 5.80 (ddd, J = 9.1, 6.0, 1.2 Hz, 2H), 5.73 (dd, J = 5.9, 1.2 Hz, 1H), 2.82 (p, J = 6.9 Hz, 1H), 2.33 (s, 3H), 1.22 (d, J = 6.9 Hz, 3H), 1.13 (d, J = 6.9 Hz, 3H). ^{13}C NMR (126 MHz, DMSO-d_6) δ 167.50, 153.30, 142.43, 136.12, 134.39, 126.93, 124.44, 110.92, 103.92, 96.21, 84.17, 82.01, 81.99, 81.31, 80.52, 31.31, 22.31, 22.11, 19.56.

*Data for **11**:* Yield (85.8%). Elemental analysis calcd (%) for $C_{20}H_{22}INORu$: C 46.16, H 4.26, N 2.69. Found: C 46.12, H 4.30, N 2.67. ESI-MS: m/z = 393.4 for $[M - Cl]^+$. ^{1}H NMR (500 MHz, DMSO-d_6) δ 8.04 (d, J = 8.5 Hz, 1H), 7.45 (d, J = 8.5 Hz, 1H), 7.13 (t, J = 7.9 Hz, 1H), 6.71 (dd, J = 7.9, 1.2 Hz, 1H), 6.65 (dd, J = 7.8, 1.1 Hz, 1H), 5.87 (dd, J = 5.8, 1.2 Hz, 1H), 5.77 (dd, J = 6.2, 1.2 Hz, 1H), 5.69 (dd, J = 6.1, 1.2 Hz, 1H), 5.47 (dd, J = 5.8, 1.2 Hz, 1H), 2.63 (td, J = 6.9, 2.5 Hz, 1H), 2.42 (s, 3H), 1.04 (d, J = 6.9 Hz, 3H), 0.92 (d, J = 6.9 Hz, 3H). ^{13}C NMR (126 MHz, DMSO-d_6) δ 168.72, 160.40, 144.58, 137.62, 128.53, 128.34, 124.17, 114.33, 109.81, 103.04, 98.66, 85.81, 81.48, 80.37, 79.94, 31.21, 30.01, 22.42, 21.91, 21.19.

*Data for **12**:* Elemental analysis calcd (%) for $C_{19}H_{20}INO_2Ru$: C 43.69, H 3.86, N 2.68. Found: C 43.67, H 3.90, N 2.66. ESI-MS: m/z = 395.4 for $[M - Cl]^+$.

Materials and methods

The X-ray crystallography structure analysis method and antitumor mechanism the detailed procedures of 13 organometallic Ru(II)-arene complexes **1**−**13** were described in ESI (supporting information).

Conclusions

A total of 13 organometallic Ru(II)-arene complexes **1**−**13** have been synthesized and characterized. Cytotoxicity studies showed that organometallic Ru(II)-arene complexes **1** and **2** have higher antiproliferative activity than other 11 Ru(II)-arene complexes on HeLa cells, with IC_{50} values 2.00 ± 0.20 nM and 25.00 ± 0.30 nM, respectively. Interestingly, all these Ru(II)-arene complexes were significantly less toxic to HL-7702 normal cells. Moreover, organometallic Ru(II)-arene complexes **1**- and **2**-induced HeLa cell apoptosis was mediated by the inhibition of telomerase activity (Fig. 11) and dysfunction of mitochondria. The organometallic Ru(II)-arene complexes **1** exhibited evident priority on antitumor activity than **2**, which should be highly associated with the key roles of the 5,7-dichloro substituted groups in L1 ligand of organometallic Ru(II)-arene complexes **1**. Remarkably, organometallic Ru(II)-arene complex **1** also evidently inhibited human cervical cells (HeLa) xenograft tumor growth (TGIR = 58.5%) in vivo. In conclusion, this study might imply the first 5,7-dihalogenated-2-methyl-8-quinolinol organometallic Ru(II)-arene complex **1** as novel Ru(II) anticancer drug candidates.

View Article Online
DOI: 10.1039/C9DT00866G

Conflicts of interest

No conflicts to declare.

Acknowledgements

We thank the National Natural Science Foundation of China (Nos. 21771043, 51572050, 21867017, 21601038, and 21261025), Guangxi Natural Science Foundation (Nos. 2016GXNSFAA380085, 2015GXNSFDA139007, and 2018GXNSFBA138021), Guangxi Key Laboratory of Electrochemical and Magnetochemical Functional Materials (EMFM20162107), the Key Foundation Project of Colleges and Universities in Guangxi (No. ZD2014108), the PhD Research Startup Program of Yulin Normal University (No. G2017009), State Key Laboratory for Chemistry and Molecular Engineering of Medicinal Resources (Guangxi Normal University) (CMEMR2018-C8 and CMEMR2017-A11) and the Innovative Team & Outstanding Talent Program of Colleges and Universities in Guangxi (2014-49) for the financial support.

References

1 I. Romero-Canelón, L. Salassa and P. J. Sadler, *J. Med. Chem.,* 2013, **56**, 1291−1300.
2 V. Novohradsky, A. Bergamo, M. Cocchietto, J. Zajac, V. Brabec, G. Mestroni and G. Sava, *Dalton Trans.,* 2015, **44**, 1905−1913.
3 K. S. M. Smalley, R. Contractor, N. K. Haas, A. N. Kup, G. E. Atilla-Gokcuman, D. S. Williams, H. Bregman, K. T. Flaherty, M. S. Soengas, E. Meggers and M. Herlyn, *Cancer Res.,* 2007, **67**, 209−217.
4 F.-Z. Sadafi, L. Massai, G. Bartolommei, M. R. Moncelli, L. Messori and F. Tadini-Buoninsegni, *ChemMedChem,* 2014, **9**, 1660−1664.
5 R. E. Morris, R. E. Aird, P. S. Murdoch, H. Chen, J. Cummings, N. D. Hughes, S. Parsons, A. Parkin, G. Boyd, D. I. Jodrell and P. J. Sadler, *J. Med. Chem.,* 2001, **44**, 3616−3621.
6 P. Nowak-Sliwinska, J. R. van Beijnum, A. Casini, A. A. Nazarov, G. Wagnières, H. van den Bergh, P. J. Dyson and A. W. Griffioen, *J. Med. Chem.,* 2011, **54**, 3895−3902.
7 L. Zeng, P. Gupta, Y. Chen, E. Wang, L. Ji, H. Chao and Z.-S. Chen, *Chem. Soc. Rev.,* 2017, **46**, 5771−5804.
8 K. J. Kilpin, S. M. Cammack, C. M. Clavel and P. J. Dyson, *Dalton Trans.,* 2013, **42**, 2008−2014.
9 T. Wilson, P. J. Costa, V. Félix, M. P. Williamson and J. A. Tomas, *J. Med. Chem.,* 2013, **56**, 8674−8683.
10 D. Sun, Y. Liu, D. Liu, R. Zhang, X. Yang and J. Liu, *Chem. Eur. J.,* 2012, **18**, 4285−4295.
11 B. Deka, T. Sarkar, S. Banerjee, A. Kumar, S. Mukherjee, S. Deka, K. K. Saikia and A. Hussain, *Dalton Trans.,* 2017, **46**, 396−409.
12 D. Havrylyuk, B. S. Howerton, L. Nease, S. Parkin, D. K. Heidary and E. C. Glazer, *Eur. J. Med. Chem.,* 2018, **156**, 790−799.
13 C. M. Santos, S. Cabrera, C. Rios-Luci, J. M. Padron, I. L. Solera, A. G. Quiroga, M. A. Medrano, C. Navarro-Ranninger and J. Aleman, *Dalton Trans.*, 2013, **42**, 13343–13348.
14 S. Tardito, A. Barilli, I. Bassanetti, M. Tegoni, O. Bussolati, R. Franchi-Gazzola, C. Mucchino and L. Marchio, *J. Med. Chem.*, 2012, **55**, 10448–10459.
15 L. Yang, J. Zhang, C. Wang, X. Qin, Q. Yu, Y. Zhou and J. Liu, *Metallomic*, 2014, **6**, 518–531.
16 M. Gobec, J. Kljun, I. Sosic, I. Mlinaric-Rascan, M. Ursis, S. Gobec and I. Turel, *Dalton Trans.*, 2014, **43**, 9045–9051.
17 B.-Q. Zou, Q.-P. Qin, Y.-X. Bai, Q.-Q. Cao, Y. Zhang, Y.-C. Liu, Z.-F. Chen and H. Liang, *Med. Chem. Commun.*, 2017, **8**, 633–639.
18 Q.-P. Qin, S.-L. Wang, M.-X. Tan, Y.-C. Liu, T. Meng, B.-Q. Zou and H. Liang, *Eur. J. Med. Chem.*, 2019, **161**, 334–342.
19 D. K. Heidary, B. Howerton and E. C. Glazer, *J. Med. Chem.*, 2014, **57**, 8936–8946.
20 H.-H. Zou, T. Meng, Q. Chen, Y.-Q. Zhang , H.-L. Wang, B. Li, K. Wang, Z.-L. Chen and F.-P. Liang, *Inorg. Chem.*, 2019, **58**, 2286−2298
21 B. J. Mulchin, C. G. Newton, J. W. Baty, C. H. Grasso, W. J. Martin, M. C. Walton, E. M. Dangerfield, C. H. Plunkett, M. V. Berridge, J. L. Harper, M. S. M. Timmer and B. L. Stocker, *Bioorg. Med. Chem.*, 2010, **18**, 3238−3251.
22 M. Kubanik, N. Y. S. Lam, H. U. Holtkamp, T. Sohnel, R. F. Anderson, S. M. F. Jamieson and C. G. Hartinger, *Chem. Commun.*, 2018, **54**, 992−995.
23 R. Cao, J.-L. Jia, X.-C. Ma, M. Zhou and H. Fei, *J. Med. Chem.*, 2013, **56**, 3636−3644.
24 C. M. Clavel, E. Păunescu, P. Nowak-Sliwinska, A. W. Griffioen, R. Scopelliti and P. J. Dyson, *J. Med. Chem.*, 2014, **57**, 3546−3558.
25 M. Gobec, J. Kljun, I. Sosič, I. Mlinarič-Raščan, M. Uršič, S. Gobec and I. Turel, *Dalton Trans.*, 2014, **43**, 9045–9051.
26 Y. Gothe, T. Marzo, L. Messori and N. Metzler-Nolte, *Chem. Eur. J.*, 2016, **22**, 12487−12494.
27 S.-W. Mao, H. Chen, L.-F. Yu, F. Lv, Y.-J. Xing, T. Liu, J. Xie, J. Tang, Z. Yi and F. Yang, *Eur. J. Med. Chem.*, 2016, **122**, 574−583.
28 J. Yan, J. Chen, S. Zhang, J. Hu, L. Huang and X. Li, *J. Med. Chem.*, 2016, **59**, 5264−5283.
29 Z.-F. Chen, Q.-P. Qin, J.-L. Qin, Y.-C. Liu, K.-B. Huang, Y.-L. Li, T. Meng, G.-H. Zhang, Y. Peng, X.-J. Luo and H. Liang, *J. Med. Chem.*, 2015, **58**, 2159−2179.
30 H. Takai, A. Smogorzewska and T. de Lange, *Curr. Biol.*, 2003, **13**, 1549−1556.
31 G. B. Celli and T. de Lange, *Nat. Cell Biol.*, 2005, **7**, 712−718.
32 Y. Zhang, D. Li, Q. Jiang, S. Cao, H. Sun, Y. Chai, X. Li, T. Ren, R. Yang, F. Feng, B.-A. Li and Q. Zhao, *Cell Death Dis.*, 2018, **9**, 743. Doi: 10.1038/s41419-018-0804-6.
33 M.-C. Wei, W.-X. Zong, E. H. Y. Cheng, T. Lindsten, V. Panoutsakopoulou, A. J. Ross, K. A. Roth, G. R. MacGregor, C. B. Thompson and S. J. Korsmeyer, *Science*, 2001, **292**, 727−730.
34 K. Sinha, J. Das, P. B. Pal and P. C. Sil, *Arch. Toxicol.*, 2013, **87**, 1157−1180.
35 Q. Zhang, Y. Teng, Y. Yuan, T. Ruan, Q. Wang, X. Gao, Y. Zhou, K. Han, P. Yu and K. Lu, *Eur. J. Med. Chem.*, 2018, **156**, 800–814.
36 A. K. P. Taggart, S.-C. Teng and V. A. Zakian, *Science*, 2002, **297**, 1023−1026.
37 Q.-P. Qin, J.-L. Qin, T. Meng, W.-H. Lin, C.-H. Zhang, Z.-Z. Wei, J.-N. Chen, Y.-C. Liu, H. Liang and Z.-F. Chen, *Eur. J. Med. Chem.*, 2016, **124**, 380−392.
38 Q. Yu, Y. Liu, J. Zhang, F. Yang, D. Sun, D. Liu, Y. Zhou and J. Liu, *Metallomics*, 2013, **5**, 222−231.
39 L. Xu, X. Chen, J. Wu, J. Wang, L. Ji and H. Chao, *Chem. Eur. J.*, 2015, **21**, 1−14.
40 K.-H. Diehl, R. Hull, D. Morton, R. Pfister, Y. Rabemampianina, D. Smith, J.-M. Vidal and C. Van De Vorstenbosch, *J. Appl. Toxicol.*, 2001, **21**, 15−23.
41 Z.-F. Chen, Q.-P. Qin, J.-L. Qin, J. Zhou, Y.-L. Li, N. Li, Y.-C. Liu and H. Liang, *J. Med. Chem.*, 2015, **58**, 4771−4789.

View Article Online
DOI: 10.1039/C9DT00866G

42 Y. Wang, J. Xiao, H.-P. Zhou, S.-L. Yang, X.-P. Wu and G. Liang, *J. Med. Chem.*, 2011, **54**, 3768−3778.
43 J.-Q. Wang, P.-Y. Zhang, L.-N. Ji and H. Chao, *J. Inorg. Biochem.*, 2015, **146**, 89–96.